

AD

AD 666767



AD 666767  
RECEIVED  
APR 12 1968  
A

Reproduced by the  
CLEARINGHOUSE  
for Federal Scientific & Technical  
Information, Springfield, Va. 22151

Watertown, Massachusetts 02172

19

ARMY MATERIALS AND MECHANICS RESEARCH CENTER

AMMRC TR 68-04

**ROOM TEMPERATURE STRENGTH OF PYROLYTIC  
GRAPHITE AS AFFECTED BY MICROSTRUCTURE  
AND BORON CONTENT**

**Technical Report by**

***SAMUEL J. ACQUAVIVA and R. NATHAN KATZ***

**February 1968**

**This document has been approved for public  
release and sale; its distribution is unlimited.**

**D/A Project 1C024401A330**

**AMCMS Code 5025.11.296**

**Ceramic Materials Research for Army Materiel  
Subtask 38075**

**ARMY MATERIALS AND MECHANICS RESEARCH CENTER  
WATERTOWN, MASSACHUSETTS 02172**

ARMY MATERIALS AND MECHANICS RESEARCH CENTER

ROOM TEMPERATURE STRENGTH OF PYROLYTIC GRAPHITE AS AFFECTED BY  
MICROSTRUCTURE AND BORON CONTENT

ABSTRACT

The strengths of pyrolytic graphites possessing four varieties of microstructure ranging from coarse-coned singularly nucleated to fine-coned continuously nucleated were examined. The fine-coned structure gave substantially higher strengths. Boron-doped pyrolytic graphite with percentages of boron varying from 0.25 to 3.3% were evaluated in terms of their modulus and flexural strength. The higher boron content material (1 to 3.3% B) achieved strengths as much as fifty percent greater than the undoped material.

## CONTENTS

	Page
ABSTRACT	
INTRODUCTION . . . . .	1
EXPERIMENTAL TECHNIQUES AND MATERIALS . . . . .	1
TEST DATA AND RESULTS	
Undoped Pyrolytic Graphite . . . . .	5
Boronated Pyrolytic Graphite . . . . .	9
SUMMARY . . . . .	11
LITERATURE CITED . . . . .	13

## INTRODUCTION

Pyrolytic graphite is considered one of the most promising materials for elevated temperature applications. As is the case with refractory metal oxides and carbides, the development of this material has been hampered by too few systematic investigations characterizing the microstructure and its effects on mechanical properties. Little work has been reported in the literature on correlations between microstructure and mechanical properties.

While the bulk of the past work has been directed at the utilization of the unique high-temperature strength and thermal properties of this material, the utilization of pyrolytic graphite at elevated temperature may be limited by its room temperature properties. As an example consider a pyrolytic graphite rocket nozzle. When the rocket is fired the stress impulse will reach the outside of the nozzle before it is at its operating temperature. To preclude premature failure of the nozzle, the material must be able to sustain the stress impulse at ambient temperature. This is a clear case of room temperature mechanical properties having the potential to limit the usefulness of a high-temperature material. For this reason, it was decided that a thorough study of the room temperature mechanical properties of pyrolytic graphite should be undertaken.

It has been shown that the microstructure of pyrolytic graphite with respect to cone size exerts a strong influence on its flexural strength.<sup>1,2</sup> Microstructure features other than cone structure may influence the room temperature flexural strength and modulus of pyrolytic graphite. For instance, indirect evidence has suggested that the crystallite size\* may correlate with these properties, and that the lamellar structure<sup>3</sup> revealed by mercury ion bombardment etching may also be related to the mechanical properties.

In addition to the effect of microstructure on the mechanical properties, the effect of boron additions was also studied since boron is known to contribute significantly to the strength of this material.<sup>4</sup> Recent advances in the technology of pyrolytic graphite production have made it possible to produce material substantially thicker than previously available deposits. Consequently, the results presented in this report represent one of the first evaluations of the mechanical properties of thick (1/4-inch) pyrolytic graphite.

## EXPERIMENTAL TECHNIQUES AND MATERIALS

From previous experimental work<sup>5</sup> it is well known that pyrolytic graphite is a highly anisotropic material, and that its strength properties in tension and compression vary considerably. To evaluate the strength-microstructure conditions for such an anisotropic material several testing techniques were considered. The uniaxial tensile test was eliminated due to the difficulty in obtaining true axial alignment between test specimen and testing machine. The flexural test was chosen since it negated any alignment problems and is fairly easy to conduct.

\*Private communication - A. Tarpinian.

In early tests in the evaluation of brittle materials, the three-point loading technique was used extensively. In this test a single load is applied to a flexural specimen supported at both ends. Analysis of this test shows that the maximum stress occurs at the point of load application. This point may not be representative of the material since there may be a critical Griffith crack<sup>6</sup> in this area, causing the measured tensile strength to be in gross error. Recognizing the possibility of such an error, the four-point loading technique was chosen for material evaluation in this study.

The four-point loading system simply consists of a bar of rectangular cross section, supported at both ends, and loaded so that the load and support points are equally spaced. The strength computed by this method provides a more representative value since the stress is measured over the area bounded by the load points.

Strain measurement is accomplished through the use of resistance-type strain gages. Both tensile and compressive strains may be measured to give some indication of anisotropy within the material.

The stress in the longitudinal fibers may be computed from the conventional flexural formula  $\sigma_t = Mc/I$  where  $\sigma_t$  = tensile stress in the bottom fibers,  $I$  = moment of inertia of the cross section,  $M$  = external moment applied to the beam, and  $c$  = one half the depth of the rectangular cross section.

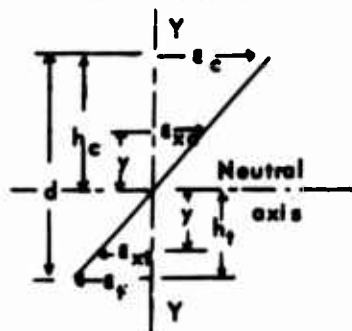
Duckworth<sup>7</sup> has proposed that a relationship between stress and strain on both the compression and tensile sides of the neutral axis, combined with the equations from the strain diagram, will permit computation of the distribution of longitudinal stress along the y axis. It is commonly accepted that in most ceramic bodies the strain is a simple linear function of stress. This is true only at low temperatures since, if the material undergoes plastic deformation, the stress-strain relation will not be linear.

Assuming a linear stress-strain relationship with the slope different in tension than in compression,

$$\sigma_t/\epsilon_t = \sigma_{xt}/\epsilon_{xt},$$

$$\sigma_c/\epsilon_c = \sigma_{xc}/\epsilon_{xc},$$

where  $\sigma_c$  and  $\sigma_t$  are unit stresses in top and bottom longitudinal fibers obtained from the accompanying strain diagram and  $\epsilon_c$  and  $\epsilon_t$  are the unit strains. The form of the strain diagram for a cross section of the gage length during bending would be



$$\frac{h_t}{d} = \frac{\epsilon_t}{\epsilon_c + \epsilon_t} \quad (1)$$

$$\frac{h_c}{d} = \frac{\epsilon_c}{\epsilon_c + \epsilon_t} \quad (2)$$

$$\epsilon_x = Ky \quad (3)$$

where  $\epsilon_t$  and  $\epsilon_c$  are the unit strains in bottom and top longitudinal fibers at a distance  $y$  from the neutral axis.

Assuming a linear stress-strain relationship with the slope different in tension than in compression,

$$\frac{\sigma_t}{\epsilon_t} = \frac{\sigma_{xt}}{\epsilon_{xt}}, \quad (4)$$

$$\frac{\sigma_c}{\epsilon_c} = \frac{\sigma_{xc}}{\epsilon_{xc}}. \quad (5)$$

From Equation 3, and the strain diagram

$$\epsilon_x = Ky,$$

$$\epsilon_t = Kh_t,$$

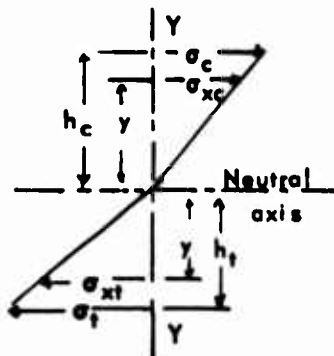
$$\epsilon_c = Kh_c.$$

Substituting these values in (4) and (5)

$$\sigma_{xt} = \frac{y\sigma_t}{h_t}, \quad (6)$$

$$\sigma_{xc} = \frac{y\sigma_c}{h_c}. \quad (7)$$

The general form of the stress diagram will be



$$\int_0^{h_t} \sigma_{xt} b y dy + \int_0^{h_c} \sigma_{xc} b y dy = M_z,$$

$$\int_0^{h_t} \frac{b \sigma_t}{h_t} y^2 dy + \int_0^{h_c} \frac{b \sigma_c}{h_c} y^2 dy = M_z,$$

$$\sigma_t h_t^2 + \sigma_c h_c^2 = \frac{3M_z}{b},$$

$$\sigma_t h_t^2 + \sigma_t h_t h_c = \frac{3M_z}{b}.$$

Replacing  $h_t$  and  $h_c$  with unit strains from (1) and (2)

$$\sigma_t = \frac{3M_z (\epsilon_c + \epsilon_t)}{bd^2 \epsilon_t}, \quad (8)$$

$$\sigma_c = \frac{3M_z (\epsilon_c + \epsilon_t)}{bd^2 \epsilon_c}. \quad (9)$$

Equation 8 gives the unit tensile stress in the bottom fibers of the flexural specimen. Similarly, (9) gives the unit compressive stress in the top longitudinal fibers.

The external moment, dimensions of the cross section of the gage length, and the unit strain in the top and bottom fibers must be known for the computations. All these quantities can be measured with considerable accuracy. For comparison with the conventional modulus-of-rupture formula  $\sigma_t = Mz/Zz$ , where  $Zz = bd^2/6$  and  $\sigma_t = 3M_z(\epsilon_t + \epsilon_c)/\epsilon_t$  and

$$\sigma_t = \frac{Mz}{Zz} \cdot \frac{\epsilon_t + \epsilon_c}{2\epsilon_t}.$$

The factor  $\frac{\epsilon_c + \epsilon_t}{2\epsilon_t}$ , therefore, is a correction factor to account for any differences between moduli of elasticity in tension and in compression.

The above relationships were utilized in a computer program to analyze the load-strain data obtained from an Instron Testing Machine and the strain instrumentation.

The four-point bend tests were performed on material machined from the flat plates with the major axis of the specimen parallel to the deposition plane; in each case the tension surface corresponded to the deposition surface. Figure 1 illustrates the specimen dimensions, orientation, and loading configuration. The load was applied through an Instron Testing Machine, with a speed of 0.002 inch per minute maintained throughout all tests.

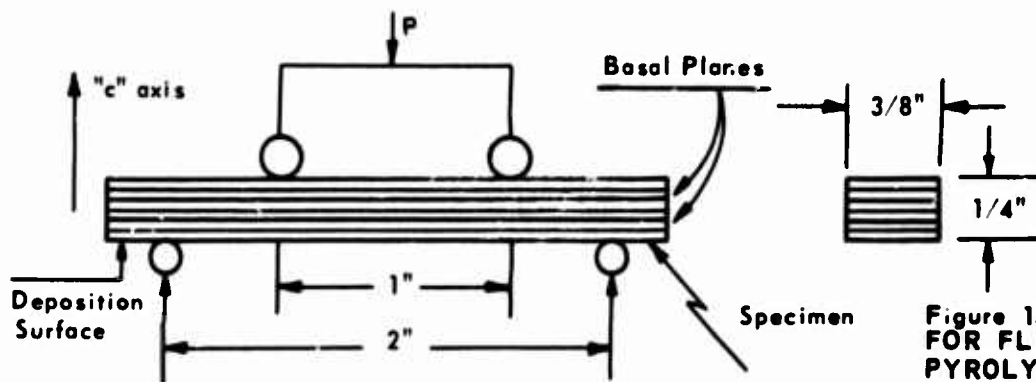


Figure 1. LOADING CONFIGURATION FOR FLEXURAL TESTING OF PYROLYTIC GRAPHITE

To measure strain, electrical resistance strain gages were mounted on the tensile and compressive faces of the specimen; the specimen was loaded in increments of ten pounds and the strain monitored for each load. Strain observations indicate a linear stress-strain relationship for this material. Typical stress-strain curves are shown in Figure 2.

The material used in this investigation was commercially available from a graphite producer. The "undoped" pyrolytic graphites were all deposited at 2000 C. Other deposition parameters were varied to provide the various cone structures shown in Figures 3a to 3c. The boron-doped materials were all deposited at 1850 C and had boron contents ranging from 0 to 3.2%. There is no apparent change in cone structure with boron content. The boron contents were the nominal compositions provided by the producer and a spectrographic analysis of the material was provided. A variance of as much as  $\pm 0.2\%$  B from the nominal is possible.

Typical microstructures of the various types of pyrolytic graphite tested are shown in Figures 3a to 3d. These microstructures are of the highly regenerative type with the degree of coarseness varying between Figures 3a, b, and c. Figure 3d shows the typical microstructure of the boron-doped pyrolytic graphite, which is singularly nucleated coarse-coned material. This structure is of a finer texture within the primary growth cone than the previous structures and was deposited at a lower temperature, 1850 C (vs. 2000 C for the undoped). Figure 3d is also typical of the undoped samples deposited at 1850 C.

## TEST DATA AND RESULTS

### Undoped Pyrolytic Graphite

The stress-strain curves obtained from the Duckworth analysis<sup>7</sup> of the load elongation data are presented in Figure 2. The moduli shown on these figures were from a least-squares analysis of the first 12 data points on the stress-strain curve including the point 0, 0 in each case. By limiting the least-square analysis to the first 12 points, it was assumed that the effect of any delamination on the modulus would be minimized. The values of E (Young's Modulus) on some of the curves do not seem to agree with the slope of the full curve. The strengths of the various types of pyrolytic graphite are compared in Table I. They are calculated from simple beam theory with no correction for a shift in the neutral axis. In Figure 3b the type A-3 microstructure is shown to have a finer primary growth cone structure. These results compare

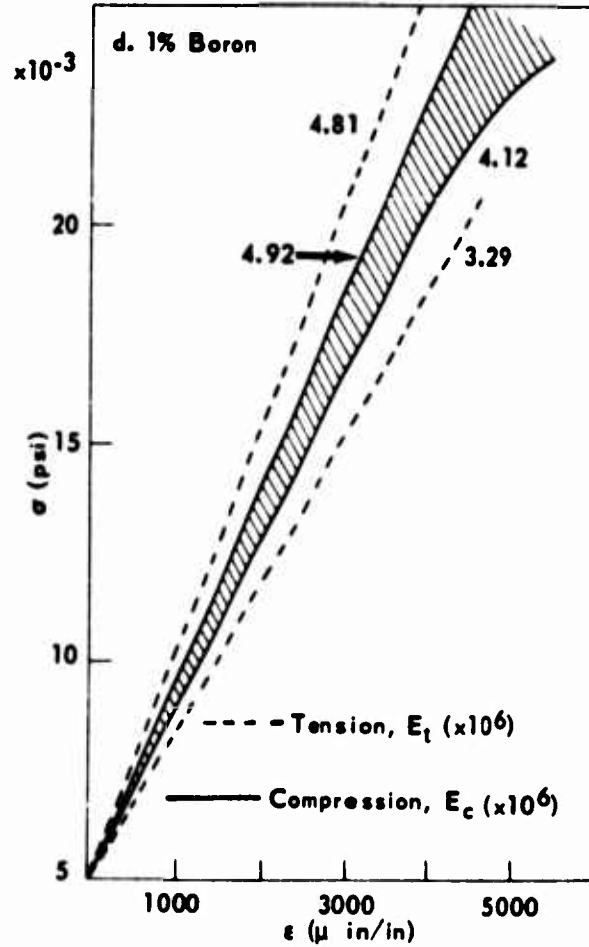
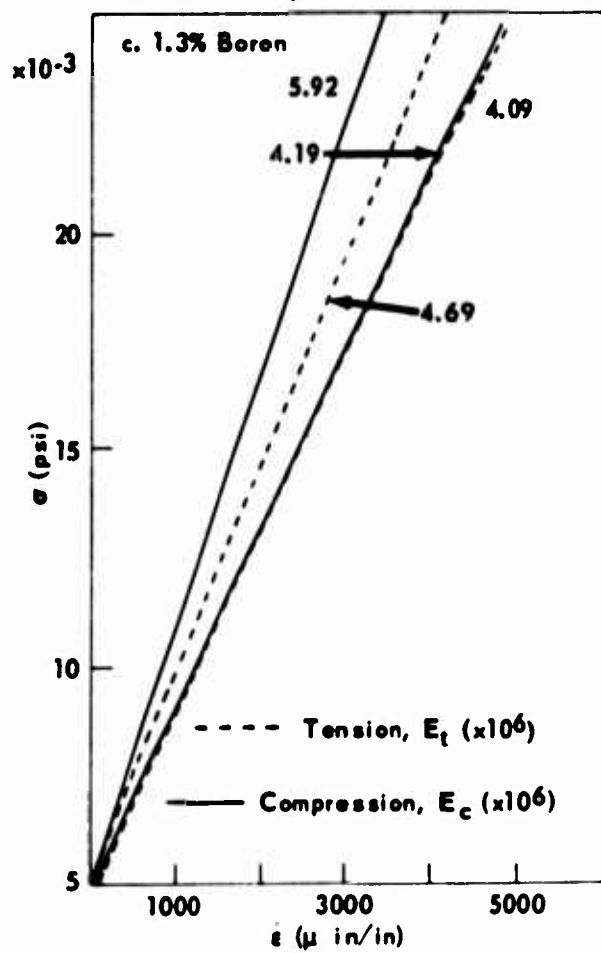
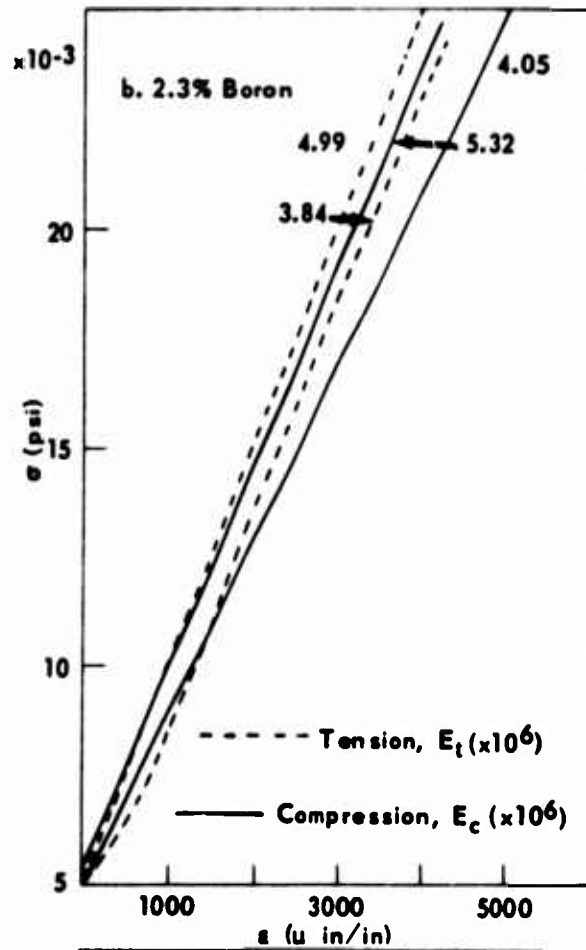
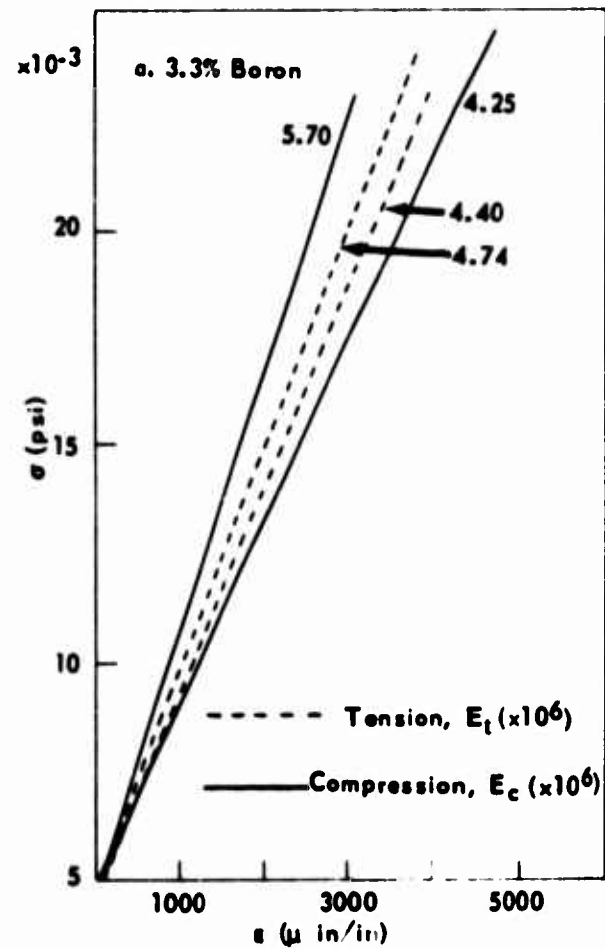


Figure 2a-d. ENVELOPE OF STRESS-STRAIN CURVES OF PYROLYTIC GRAPHITE

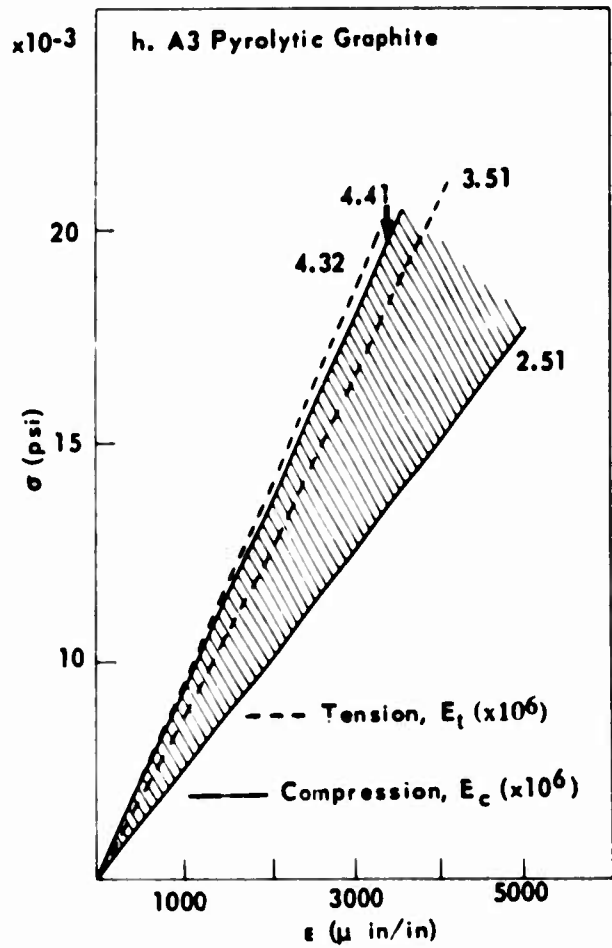
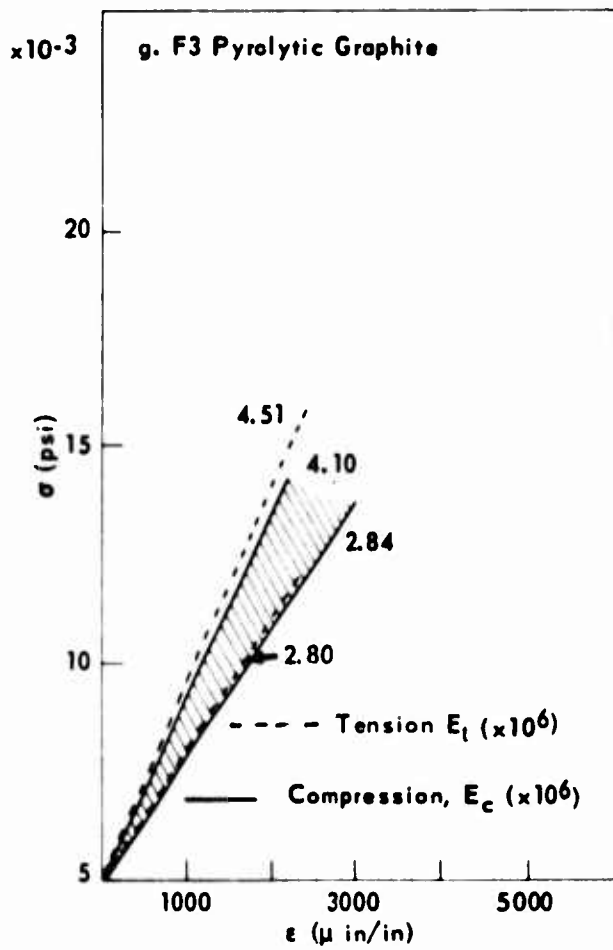
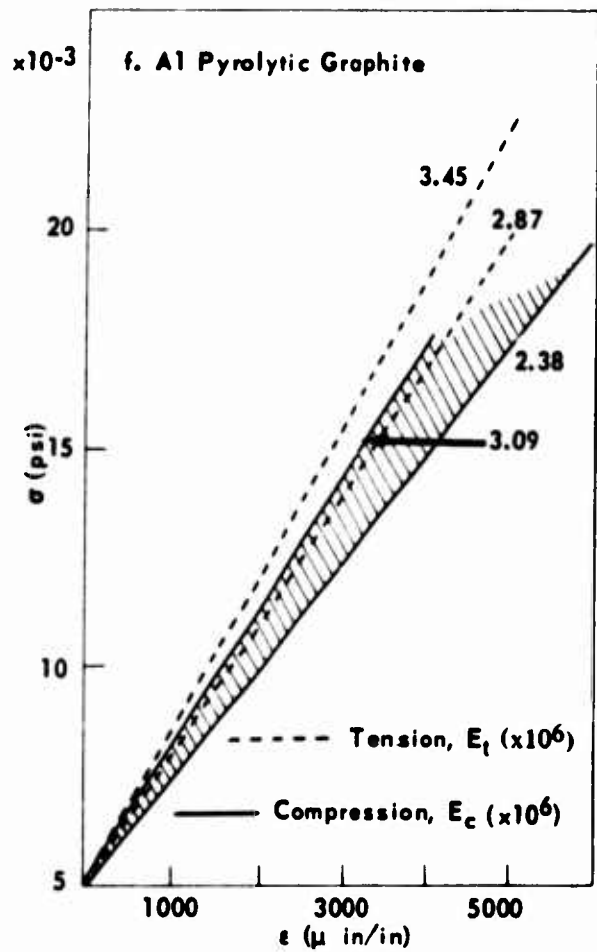
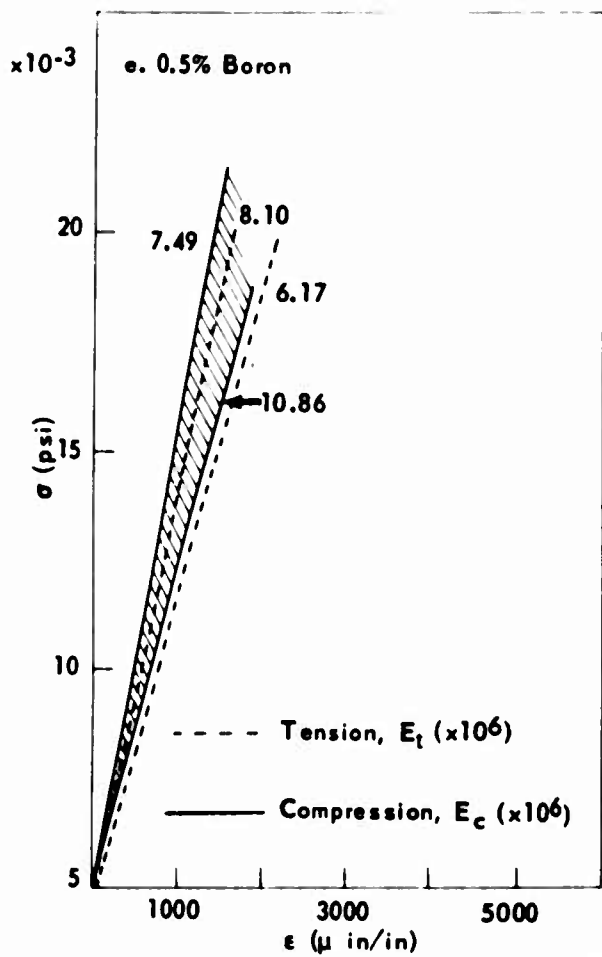


Figure 2e-h. ENVELOPE OF STRESS-STRAIN CURVES OF PYROLYTIC GRAPHITE



Type F3 - 2000 C Deposition Temperature



Type A3 - 2000 C Deposition Temperature



Type A1 - 2000 C Deposition Temperature



All Boron-Doped - 1850 C Deposition Temperature

Figure 3. TYPICAL MICROSTRUCTURES OF PYROLYTIC GRAPHITE  
Mag. 100X - Polarized Light

favorably with the data of Donadio and Pappis<sup>1</sup> who also found that continuously nucleated material had a higher strength. It should be noted that the size effect\* so often encountered in brittle materials is rather large for pyrolytic graphite. A previous investigator<sup>1</sup> used a beam 0.15 x 0.15 inch in cross section (0.0225 sq. in.) whereas this study used a 0.25 x 0.375 inch cross section (0.09375 sq. in.). Thus, if no size effect were operative, it would be expected that the larger specimens might carry four times the stress that the smaller specimens could carry. However, the larger specimens were actually one third weaker than the smaller ones, 18 to 14 ksi versus 24 to 18 ksi, respectively. This large size effect is probably due to the increase in residual stresses, delaminations, and microcracks one encounters in the thicker deposits superimposed on the normally expected purely geometric size effect.

A typical fracture for the undoped pyrolytic graphite is shown in Figure 4. It can be seen that the fracture occurs at the primary growth cone boundaries. The undoped specimens fractured along shear planes, i.e., approximately 45 degrees to the major axis of the flexure specimen, with the fracture path preferring the growth cone boundaries.



Figure 4. FRACTURE IN TYPE F3 PYROLYTIC GRAPHITE. Mag. 50X, polarized light. Typical of all fractures of undoped pyrolytic graphite deposited at 2000 C. Note fracture occurring at primary growth cone boundary.

The values of Young's Modulus of the undoped pyrolytic graphites tested in this study are presented in Table I. For this material it is evident that the higher strength materials at a given deposition temperature have a higher flexural modulus. However, either deposition temperature or microstructure, or both, cause the singularly nucleated material deposited at 1850 C to have the highest modulus. There is not the same relationship between microstructure and modulus as there is between microstructure and strength. It is also apparent that the value of E is higher in tension than in compression. These values are the average of 4 to 5 specimens and in each group one or two specimens had the opposite behavior, that is, E was higher in compression. This variation in behavior between specimens is most likely the result of delaminations or microcracks in the material relieving local stresses near the strain gages.

#### Boronated Pyrolytic Graphite

The second phase of this program was to determine the effect of boron

\*The size effect states that as one increases the diameter of the test piece the strength will decrease. The effect is usually rationalized on the basis of Griffith's crack theory.

Table I. FLEXURAL STRENGTH AND MODULUS OF PYROLYTIC GRAPHITE MICROSTRUCTURES

Type of Structure	Tensile Strength, ksi	Error, ksi	Young's Modulus, psi	
			Tension	Compression
A3	18.07	±2.2	$3.81 \times 10^{-6}$	$3.45 \times 10^{-6}$
F3	16.98	±1.9	3.70	3.15
A1	14.55	±2.0	3.17	2.71
Coarse cone 1850 C Dep.	14.270	±1.5	5.55	5.37

doping on the strength of the pyrolytic graphite. Flexural specimens were cut from plates containing boron percentages varying from 0.25 to 3.3. Data from these tests plotted in Figure 5 indicate that the maximum strength occurs when the boron content is in the area of 1.0% to 3.0%. A slight drop in strength

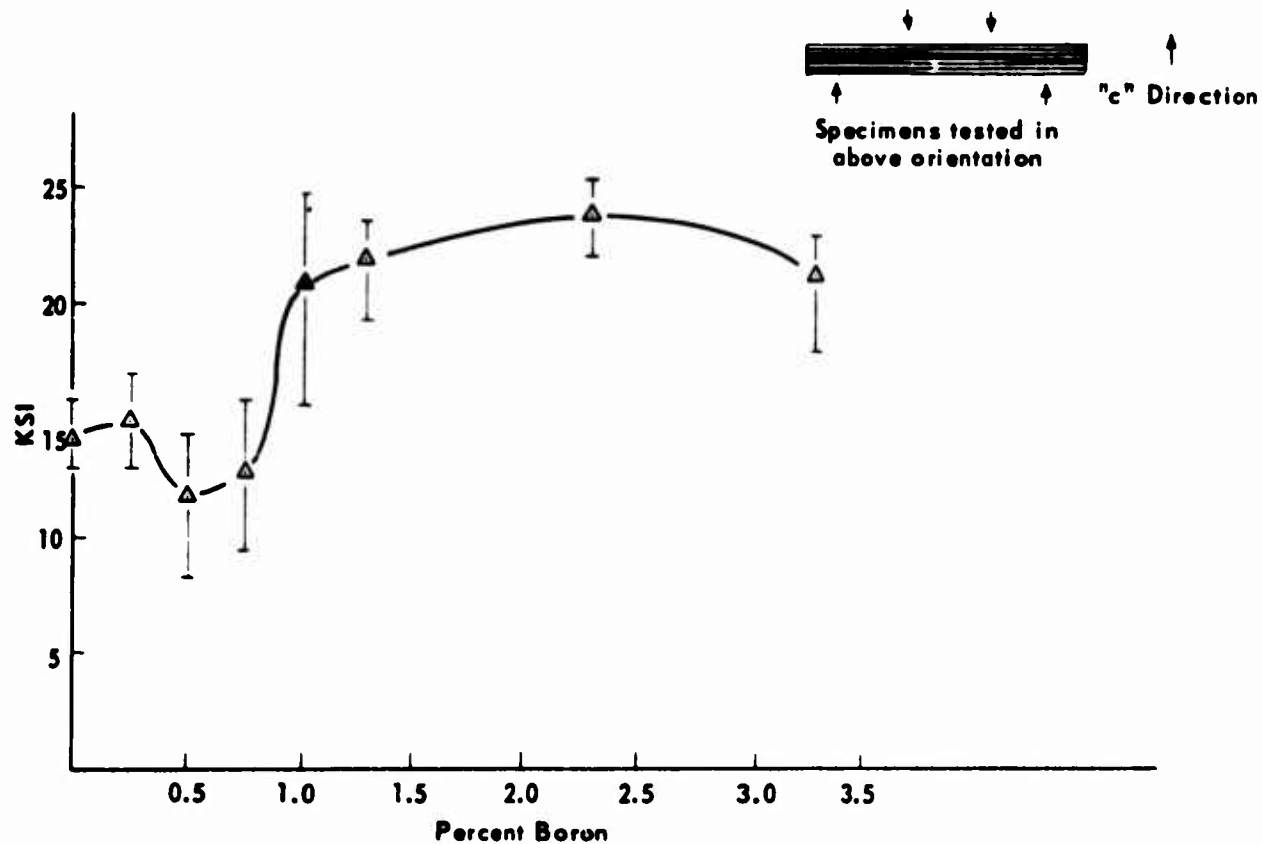


Figure 5. FLEXURAL STRENGTH OF BORONATED PYROLYTIC GRAPHITE VERSUS BORON CONTENT IN WEIGHT PERCENT

is encountered at 3.3% boron. One phenomenon noted with the boron-doped material with 0.5% to 0.75% boron was that the strength decreased significantly. Additional specimens were tested from the 0.5% boron material to confirm this effect. Strength increases of as much as 50 percent were obtained with the higher boron content material (2.3% B) over the undoped material. The stress-strain curves for the boron content material are shown in Figures 2a through e together with the average elastic modulus. The strain gage data indicates that the stress-strain curves are linear. Table II presents data on the average strength and average modulus.

Table II. FLEXURAL STRENGTH AND MODULUS OF BORONATED PYROLYTIC GRAPHITE

Boron, %	Flexural Strength in Tension, psi	Modulus, psi	
		Tension	Compression
0	14,270	$5.55 \times 10^{-6}$	$5.37 \times 10^{-6}$
0.25	15,080	--	--
0.50	11,600	8.04	8.11
0.75	12,650	--	--
1.00	20,750	4.00	4.51
1.30	22,000	4.45	5.03
2.3	23,800	4.52	4.86
3.3	21,200	4.57	4.75

Fracture behavior of the boron-doped material was different than that of the undoped material. These specimens developed shear delaminations parallel to the deposition planes or "a" direction. Due to these delaminations, full fracture into two or more separate pieces was seldom encountered in the boron-doped material. The strengths of these specimens were calculated from the maximum load rather than load at fracture.

The average modulus of the boronated pyrolytic graphites was higher for all boron compositions in compression rather than in tension. This is particularly interesting since from Table I it can be seen that if no boron is present the moduli are higher in tension. No explanation for this behavior is offered, other than to speculate that such behavior may be related to the presence of  $B_4C$  deposit (and the resultant lattice strains) recently suggested as a mechanism to explain the effect of boron on the fine microstructure of pyrolytic graphite.<sup>8</sup>

#### SUMMARY

The strength of undoped pyrolytic graphite may be varied according to the microstructure of the material. The finer cone structure material yields significantly higher strengths than the coarse structure material.

By the addition of boron to the pyrolytic graphite during deposition, further increase in strength may be realized. The highest strength is obtained when the boron content ranges between 1.0 and 3.0%. Increases in strength of as much as fifty percent over undoped material are noted with the addition of the above amount of boron.

Fracture in the undoped material occurs primarily along the cone boundary, and in the boron-doped material fracture occurs as shear along the basal planes.

A large size effect is encountered in undoped pyrolytic graphite which results in a severe degradation in the flexural strength as the specimen thickness increases.

Moduli of elasticity measured in flexure in pyrolytic graphite vary with the nature of the stress. In the case of undoped material the average modulus is greater in tension, whereas doping causes the modulus in compression to be higher. It has also been shown that the relationship between microstructure and modulus is not as direct as between microstructure and strength.

## LITERATURE CITED

1. DONADIO, R. N., and PAPPIS, J. *The Mechanical Properties of Pyrolytic Graphite*. Raytheon Tech. Mem. T 574, May 1964.
2. GEBHART, J. J., and BERRY, J. M. *Mechanical Properties of Pyrolytic Graphite*. AIAA Journal 3(2) 1965, p. 302-308.
3. TARPINIAN, A. *Electrochemical and Ion Bombardment Etching of Pyrolytic Graphite*. Journal of American Ceramics Society, v. 47, p. 532.
4. PAPPIS, R., DONADIO, R. N., HAGEN, L. M., and CAPRIULO, A. J. *The Properties of Boron-Doped Pyrolytic Graphite*. Presented at the 2nd ASTM Symposium on Pyrolytic Graphite Materials, Palm Springs, May 10-11, 1966.
5. PAPPIS, J., and BLUM, S. *Properties of Pyrolytic Graphite*. Journal of American Ceramics Society, v. 44, No. 9, September 1961, p. 592.
6. TETELMAN, A. S., and McEVILY, A. J. *Fracture of Structural Materials*. J. Wiley, New York, 1967, p. 50.
7. DUCKWORTH, W. H. *Precise Tensile Properties of Ceramic Bodies*. Journal of American Ceramics Society, January 1, 1951.
8. KATZ, R. N., and GAZZARA, C. P. *The Fine Microstructure of Pyrolytic Graphite as Influenced by Boron*. Army Materials and Mechanics Research Center, AMRC TR 68-02, January 1968.

DOCUMENT CONTROL DATA - R&D		
<i>(Security classification of title, body of abstract and indexing annotation must be entered when the overall report is classified)</i>		
1. ORIGINATING ACTIVITY (Corporate author) Army Materials and Mechanics Research Center Watertown, Massachusetts 02172		2a. REPORT SECURITY CLASSIFICATION Unclassified
		2b. GROUP
3. REPORT TITLE ROOM TEMPERATURE STRENGTH OF PYROLYTIC GRAPHITE AS AFFECTED BY MICROSTRUCTURE AND BORON CONTENT		
4. DESCRIPTIVE NOTES (Type of report and inclusive dates)		
5. AUTHOR(S) (Last name, first name, initial) Acquaviva, Samuel J. and Katz, R. Nathan		
6. REPORT DATE February 1968	7a. TOTAL NO. OF PAGES 13	7b. NO. OF REFS 8
8a. CONTRACT OR GRANT NO	9a. ORIGINATOR'S REPORT NUMBER(S) AMMRC TR 68-04	
b. PROJECT NO D/A 1C024401A330		
c. AMCMS Code 5025.11.296	9b. OTHER REPORT NO(S) (Any other numbers that may be assigned this report)	
d. Subtask 38075		
10. AVAILABILITY/LIMITATION NOTICES This document has been approved for public release and sale; its distribution is unlimited.		
11. SUPPLEMENTARY NOTES	12. SPONSORING MILITARY ACTIVITY U. S. Army Materiel Command Washington, D. C. 20315	
13. ABSTRACT The strengths of pyrolytic graphites possessing four varieties of microstructure ranging from coarse-coned singularly nucleated to fine-coned continuously nucleated were examined. The fine-coned structure gave substantially higher strengths. Boron-doped pyrolytic graphite with percentages of boron varying from 0.25 to 3.3% were evaluated in terms of their modulus and flexural strength. The higher boron content material (1 to 3.3% B) achieved strengths as much as fifty percent greater than the undoped material. (Author)		

14 KEY WORDS	LINK A		LINK B		LINK C	
	ROLE	WT	ROLE	WT	ROLE	WT
Flexural strength Inorganic material Modulus of elasticity Microstructure Nucleation Tensile stress Compressive stress Anisotropy						

INSTRUCTIONS

1. **ORIGINATING ACTIVITY:** Enter the name and address of the contractor, subcontractor, grantee, Department of Defense activity or other organization (*corporate author*) issuing the report.

2a. **REPORT SECURITY CLASSIFICATION:** Enter the overall security classification of the report. Indicate whether "Restricted Data" is included. Marking is to be in accordance with appropriate security regulations.

2b. **GROUP:** Automatic downgrading is specified in DoD Directive 5200.10 and Armed Forces Industrial Manual. Enter the group number. Also, when applicable, show that optional markings have been used for Group 3 and Group 4 as authorized.

3. **REPORT TITLE:** Enter the complete report title in all capital letters. Titles in all cases should be unclassified. If a meaningful title cannot be selected without classification, show title classification in all capitals in parenthesis immediately following the title.

4. **DESCRIPTIVE NOTES:** If appropriate, enter the type of report, e.g., interim, progress, summary, annual, or final. Give the inclusive dates when a specific reporting period is covered.

5. **AUTHOR(S):** Enter the name(s) of author(s) as shown on or in the report. Enter last name, first name, middle initial. If military, show rank and branch of service. The name of the principal author is an absolute minimum requirement.

6. **REPORT DATE:** Enter the date of the report as day, month, year; or month, year. If more than one date appears on the report, use date of publication.

7a. **TOTAL NUMBER OF PAGES:** The total page count should follow normal pagination procedures, i.e., enter the number of pages containing information.

7b. **NUMBER OF REFERENCES:** Enter the total number of references cited in the report.

8a. **CONTRACT OR GRANT NUMBER:** If appropriate, enter the applicable number of the contract or grant under which the report was written.

8b, 8c, & 8d. **PROJECT NUMBER:** Enter the appropriate military department identification, such as project number, subproject number, system numbers, task number, etc.

9a. **ORIGINATOR'S REPORT NUMBER(S):** Enter the official report number by which the document will be identified and controlled by the originating activity. This number must be unique to this report.

9b. **OTHER REPORT NUMBER(S):** If the report has been assigned any other report numbers (*either by the originator or by the sponsor*), also enter this number(s).

10. **AVAILABILITY/LIMITATION NOTICES:** Enter any limitations on further dissemination of the report, other than those imposed by security classification, using standard statements such as:

- (1) "Qualified requesters may obtain copies of this report from DDC."
- (2) "Foreign announcement and dissemination of this report by DDC is not authorized."
- (3) "U. S. Government agencies may obtain copies of this report directly from DDC. Other qualified DDC users shall request through \_\_\_\_\_."
- (4) "U. S. military agencies may obtain copies of this report directly from DDC. Other qualified users shall request through \_\_\_\_\_."
- (5) "All distribution of this report is controlled. Qualified DDC users shall request through \_\_\_\_\_."

If the report has been furnished to the Office of Technical Services, Department of Commerce, for sale to the public, indicate this fact and enter the price, if known.

11. **SUPPLEMENTARY NOTES:** Use for additional explanatory notes.

12. **SPONSORING MILITARY ACTIVITY:** Enter the name of the departmental project office or laboratory sponsoring (*paying for*) the research and development. Include address.

13. **ABSTRACT:** Enter an abstract giving a brief and factual summary of the document indicative of the report, even though it may also appear elsewhere in the body of the technical report. If additional space is required, a continuation sheet shall be attached.

It is highly desirable that the abstract of classified reports be unclassified. Each paragraph of the abstract shall end with an indication of the military security classification of the information in the paragraph, represented as (TS), (S), (C), or (U).

There is no limitation on the length of the abstract. However, the suggested length is from 150 to 225 words.

14. **KEY WORDS:** Key words are technically meaningful terms or short phrases that characterize a report and may be used as index entries for cataloging the report. Key words must be selected so that no security classification is required. Identifiers, such as equipment model designation, trade name, military project code name, geographic location, may be used as key words but will be followed by an indication of technical context. The assignment of links, rules, and weights is optional.